Hydrophilic Surfaces Turning of Graphene Nano Platelets by 1,3,6-Trihydroxyxanthone: π–π Stacking Interaction Affair in 2-D

Emmy Yuanita*, Sirojuttolibin Sirojuttolibin, Ni Komang Tri Dharmayani, Maria Ulfa, Maulida Septiyana, and Sudirman Sudirman

Department of Chemistry, Faculty of Mathematics and Natural Sciences, University of Mataram, Jl. Majapahit No. 62, Mataram 83115, Indonesia

** Corresponding author:*

email: emmy_yuanita@unram.ac.id

Received: October 18, 2023
Accepted: March 12, 2025

DOI: 10.22146/ijc.89894

Abstract: *Graphene nanoplatelet (GNP) has a good potential to be developed as a drug carrier material. In this study, the interaction of GNP with one type of drug, namely 1,3,6-trihydroxyxanthone (THX), has been studied. The results of XRD analysis and FTIR uptake show an excellent interaction between THX and GNP through the π–π stacking channel. This interaction makes the GNP surface more polar and soluble in the aqueous media. THX-graphene shows physical and chemical stabilities, where THX can be released under specific and controlled conditions. The results of this study show the potential of utilizing graphene as a drug carrier material for more specific disease targets with a longer drug release time.*

Keywords: *trihydroxyxanthones; graphene; π–π stacking; polar surfaces*

■ INTRODUCTION

Graphene (G) is an allotrope of carbon, a nanomaterial which is claimed to be a two-dimensional material. Thus, G has many unique characteristics, such as a large surface area and high thermal conductivity. Therefore, in the last few decades, G has attracted many researchers' attention to investigate its potential applications. Currently, G is not only applied in various technologies such as electronic systems [1], solar cells [2], capacitors [3], batteries [4], but also widely applied in biological systems such as biomaterial for bone replacement [5], bio-membrane penetration [6], tumor therapy, and theragnostic [7], and material for drug delivery system [8] due to its biocompatible and non-toxic properties. In particular, application as drug delivery material, considering the toxicity of the introductory material and the form of interaction involved between the drug and the delivery material, is incredibly essential. These will be related to drug-loaded, control realization, and stability of the drug and its delivery system [9].

G is mostly synthesized from graphite through a chemical exfoliation process to produce graphene oxide (GO). In comparison, the case with G, where almost all the constituent carbon is sp^2 hybridization, which causes G to be hydrophobic, in GO, carbon is in sp^2 and sp^3 formation, and the presence of oxygen atoms in various forms of functional groups causes GO to be hydrophilic [10]. Moreover, the existence of functional groups containing oxygen atoms could lead to the formation of strong covalent bonds while interacting with drug molecules. Therefore, it is difficult to control the drug release because it requires a large amount of energy to break the covalent bond. So, the use of reduced graphene oxide (rGO) or G is preferred, although it requires a functionalization process as needed. However, The G's functionalization process, which does not involve the formation of covalent bonds, is in favor, which involves π–π interaction, van der Waals, ionic interaction, and hydrogen bond [11]. Several previous studies have successfully functionalized noncovalent interactions with polyethylene glycol (PEG) polymers [12], glucose oxidase biomolecules [13], Ramizol drug [14], 3D superstructure such as pyrene derivates as linkers [15], and carbon nano allotrope such as single walls nanotube (SWNT) [16]. However, using macromolecules to decorate G will drastically increase the mass of the carrier material. Although this can improve the mechanical properties of

the drug carrier material, a center of mass that is too large will reduce the mobility during drug delivery to the target, thereby reducing the effectiveness of the drug.

Therefore, in this study we proposed an exciting interaction between G and 1,3,6-trihydroxyxanthones (THX). Xanthone and its derived compound have been widely developed as a therapeutic drug for antioxidant [17], anticancer [18], antibacterial [19], and antimalarial [20]. An interesting result was observed that THX adsorbed on the graphene nanoplatelet (GNP) surface caused GNP to be hydrophilic, whereas previously, GNP was hydrophobic and insoluble in water. This change from hydrophobic to hydrophilic of GNP-THX is very important because of the application of biology, where the processes that occur in the body are in the aqueous media. Water solubility and lipophilicity influence the dissolution of drugs and the ultimate free drug concentration since they determine the ability of the drug to dissolve in and move through cell membranes and distribute throughout the body. Since water solubility, lipophilicity, and permeability are important parameters in estimating drug absorption properties *in vivo* [21]. In addition, the types of interactions that are formed are then tested for physical and chemical stability in relation to drug realization as a consideration in formulating THX with a carrier material in the form of GNP as a drug.

■ EXPERIMENTAL SECTION

Materials

GNP powder was purchased from Sigma Aldrich. Benzoic acid, resorcinol, phloroglucinol, Eaton reagent (P_2O_5/CH_3SO_3H), ethanol, ammonium nitrate, potassium hydrogen sulphate, nitric acid, sulfuric acid, and dimethyl sulfoxide (DMSO) were obtained from Merck and used in the synthesis of THX.

Instrumentation

The initial identification and reaction monitoring of synthesis of THX was determined by thin layer chromatography (TLC). Moreover, the structure elucidation and the changes in the morphological structure of GNP was carried out using FTIR (Shimadzu Prestige 21) and XRD (PANalytical, type X'Pert PRO).

Procedure

Synthesis of THX

The synthesis of THX was carried out by modifying the procedure performed by Yuanita et al. [17] from 3 h to 30 min, which remained using benzoic acid and phenol derivatives as primary precursors. A mixture of resorcinol acid, phloroglucinol, and Eaton reagent in a ratio of 1:1:1, respectively, were added into a three-neck flask and heated at about 80 °C for 30 min. After the reaction, the reactor was cooled to room temperature and then poured into ice water until a precipitate was formed. Next, the precipitate formed was stirred for 1 h, followed by filtration and washed with distilled water. The final product was dried in a desiccator for 24 h.

Physical adsorption of THX onto GNP

THX was dissolved into ethanol in various concentrations (20, 40, 60, 80, 120 ppm, and until saturated). Each 6 mL of THX solution was added with 6 mg of GNP and stirred in an ultrasonic bath for 5 min. The mixture was then separated by centrifuge. The precipitate was stored and then dried.

Characterization

The morphology changes in GNP that had adsorbed THX were determined using XRD (PANalytical) with a single scan measurement type and Reflection measurement mode ($K_{\alpha1}$ = 1.54060; $K_{\alpha2}$ =1.54430, K_{β} = 1.39225, $K_{\alpha1}/K_{\alpha2}$ = 0.50000). The vibration mode that appears in the GNP-THX sample was also observed using FTIR in ambient conditions.

Physical stability

A physical stability test was investigated by dissolving a number of GNP-THX samples into distilled water then placed in a sonic bath for 1, 2, 3, 4, and 5 min and lastly left for 24 h.

Chemical stability

The chemical stability test was carried out by dispersing several GNP-THX samples in a solution with a pH of 2, 4, 6, 8, 10, and 12, respectively. Next, it was placed in a sonic bath for 5 min, then allowed at room temperature for 24 h.

■ RESULTS AND DISCUSSION

The Effect of THX Adsorption on GNP

G, as has been claimed to be a two-dimensional nanomaterial, has a large surface area and is highly reactive. This unique property is not only due to its dimensions but also because of the anomaly of electron behavior as it is on a metal surface. The type of G that is synthesized and used in this study is GNP, while the xanthone derivative that interacts with G is THX. The basal plane of G is a two-dimensional plane with a large surface area. Generally, molecular interaction activity on G occurs at the edges because the basal plane tends to have low affinity, so it takes a lot of energy to form an active layer on its surface [22]. However, molecules with aromatic rings will have great compatibility on this basal surface due to the electronic effect on the conjugated system [1], so G material can be used as a more specific carrier material for the type of drug molecules with large aromatic rings.

Based on the computational geometry optimization with the DFT method on the basis of the BL3LYP (Gaussian09®) set with ethanol solvent, THX shows a conformation with minimum energy, i.e., all the atoms are in a plane (Fig. 1). The same thing was reported in previous studies [23]. In contrast to the case reported for isogenticin (1,3-dihydroxy-7-methoxyxanthone), which is also a xanthone derivative where even though all the atoms are in one plane, the hydrogen atoms of the methyl group are in the tetrahedral geometry, so they are not in one plane. With the main structure, this can cause a certain distance for the two structures to be able to interact with each other in π–π stacking [24]. In addition, the three rings in the THX structure are connected to the π-conjugate system, and they build its geometry structure. Therefore, the requirement for π–π stacking interaction is fulfilled [10].

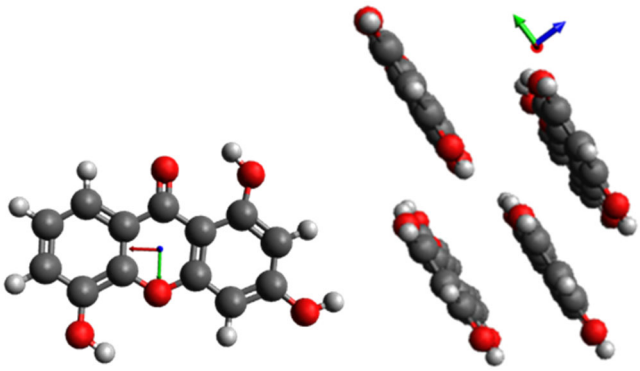

Fig 1. An optimized of THX molecule where all the atoms are in one plane

Physical adsorption was performed to study the interaction between G and THX. After THX is dissolved with ethanol in various concentrations, a constant mass amount of G is added to the solution. The THX in which adsorbs by G is measured by XRD, although many researchers consider it challenging to study G structures using XRD. Because G theoretically will be in a single-layer condition, there will be no parallel diffraction plane. Although, many researchers still use XRD to study allotropes of crystalline carbon, such as graphite, G, and diamond. Nevertheless, for GNP since GNP has a layer containing both electron-rich and electron-poor regions, it will not be easy to interact well with all aromatic compounds. Thus, not only the aromaticity of the molecule takes into account the electron-donor or electron attractors [23], but also substituents [25], size, and planarity [11].

As shown in Fig. 2, the peak at an angle of 2θ around 26.4° is a characteristic of graphite which shows the distance between the carbon layers, while it presents the (002) reflection. Even in the standard GNP sample

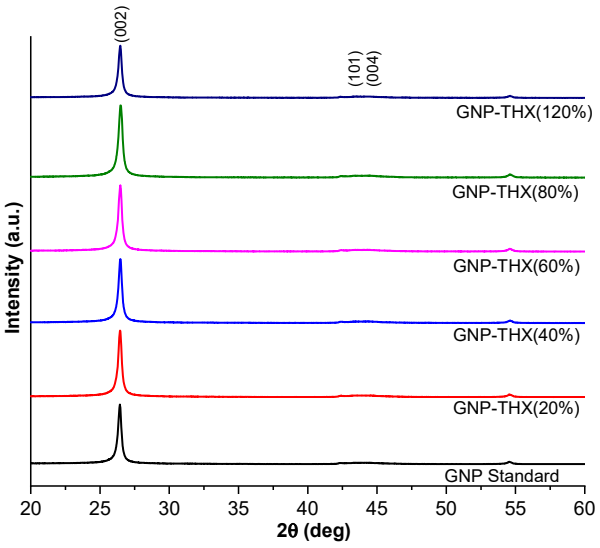

Fig 2. The GNP XRD pattern changes according to the increase in the number of THX molecules

used, the (002) reflection still exists with a high enough intensity. Based on these results, we can say that the standard GNP used is still present in several layers, which gives a high (002) reflection. Samples with low THX composition levels did not show a significant change in diffraction intensity in the d-spacing (002) field (Fig. 2). This means the small amount of THX adsorption does not change the crystallinity of the standard G significantly. It is easily understood because the ratio of the size of the G is very large in a wide 2D form. The THX molecules will be able to cover a small part of the G's surface.

In contrast, the GNP sample saturated with THX solution, where the diffraction peak density of the (002) reflection dropped drastically (Fig. 3). It illustrates that the graphite characteristics are decreasing while the characteristics of the G are increasing by decreasing crystallinity [26]. The explanation of this trend is the higher the peak density of the d plane (002), the more identical parallel planes that diffract the X-rays, and subsequently, the number of carbon layers increases. On the other hand, if the peak intensity of the (002) reflection decreases, the less identical parallel planes diffract from the light. Moreover, the fewer carbon layers are formed. It is also possible to insert a G interlayer, which causes the G to split into several thinner layers. This is possible because the interconnection caused by the van der Waals forces of THX is preferred because of the difference in electron density of the two systems, which weakens the interaction between the G layers [27]. By using Brag's law (Eq. (1)), the distance between layers (d-002) based on an angle of 2θ is about 26°, and it gives a d spacing value of 3.35–3.37 Å, which is in accordance with typical G obtained from expansion graphite [28]. The value of d(002) for spacing also indicates π–π interaction between layers, which occurs in a face-to-face perfect alignment [29]. The same is true for the peaks at angles of 44.8° d(101) and 54.9° d(004) (Fig. 3). All the diffraction peaks of the GNP-THX are also compared to the JCPDS Card No.00-012-0212.

$$nd = 2d_{hkl} \sin\theta \quad (1)$$

To further analysis, changes in the size of the G layer are generally done by analyzing aromatic C–C vibrations in the basal plane and edge sites. The smaller the G layer,

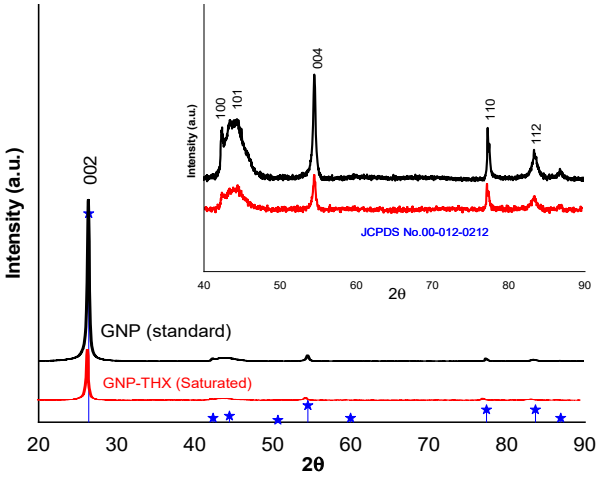

Fig 3. The XRD Pattern of GNP, GNP-THX (saturated) and π-π interaction between them

the more the intensity of C–C vibrations in the basal plane will increase. The analogy with this, by observing the intensity of XRD by the d(002) plane decreasing (with identical measurements), it can be interpreted that the G layer is decreasing. The decrease in the number of GNP layers after adsorbing THX to saturation can be seen from the crystallite size (D) of the material, which can be calculated based on Scherrer's equation (Eq. (2)). Where K is a dimensionless shape factor, with a value close to unity, the shape factor has a typical value of about 0.9 but varies with the actual shape of the crystallite; λ is the X-ray wavelength (1.5406 nm); β is the line broadening at half the maximum intensity (FWHM), after subtracting the instrumental line broadening, in radians. This quantity is also sometimes denoted as Δ(2θ), and θ is the Bragg angle. The change in crystallite was then plotted against the concentration of THX shown in Fig. 4. Based on Fig. 4, it can be seen that the initial crystallite of the standard GNP is around 54.2599 nm, which then decreases to 33.2237 nm when the THX concentration reaches 120%. The contrast occurred when the GNP was saturated with THX, where the size of the crystallite was reduced to half the initial size of 28.974 nm. This is probably due to splitting the GNP layer into two or more with almost the same size average. This change causes GNP-THX (saturated) to become hydrophilic and stable on the aqueous medium.

$$D = \frac{K\lambda}{\beta\cos\theta} \quad (2)$$

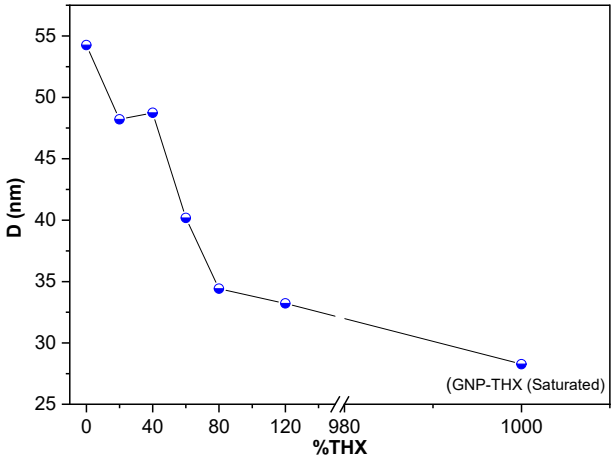

Fig 4. Change in crystallite size from GNP-THX vs. THX concentration

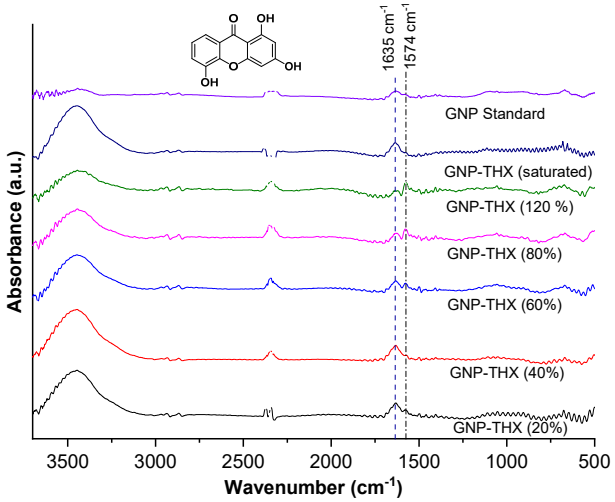

Fig 5. The FTIR spectra of GNP changes according to the increase in the number of THX molecules

The other evidence that a good interaction is formed between THX and GNP is also seen in the FTIR spectrum (Fig. 5), where the absorption is strong and broad in the wavenumber region of 3600–3200 cm^{-1}, which is the stretching of the hydroxyl groups of the THX molecule. The strong and broad absorption could also indicate that the hydroxyl functional groups in THX are in the free and exposed condition with the GNP plane. Moreover, the absorbance intensity of this peak increases as the concentration of THX in GNP increases. However, another circumstance may occur to the carbonyl group on THX that was not observed. The peak at the wave number 1635 cm^{-1} is not significant enough to be claimed as a vibrational form of the THX carbonyl group. It is possible because the carbonyl group on THX is part of the conjugated system of the THX molecule; therefore, what is assessable is the aromatic carbon bending associated with the conjugated system at GNP, which is more likely to be determined as a peak at the wave number 1635 cm^{-1} [30].

It is interesting that the absorption peak is around 1630–1570 cm^{-1}, whereas the GNP standard only shows one absorption peak at 1635 cm^{-1}, which is probably the vibrational mode of C=C aromatic *in-plane* from GNP. When THX is 20%, a new peak appears at 1574 cm^{-1}, where this peak has an absorption value that continues to increase until the THX 60% absorption is almost the same as the peak of 1635 cm^{-1}. Meanwhile, when the THX concentration was 80–120%, the absorption peak of 1547 cm^{-1} exceeded the peak of 1635 cm^{-1}. This shows that both GNP and THX are still visible. A contrast was observed when GNP-THX was saturated, wherein anywhere around 1630–1570 cm^{-1} returned to unity. This may occur when the GNP layer has undergone splitting, the interaction is getting stronger, and in the same vibration mode between the aromatic ring from GNP and THX through phi-phi stacking interaction. However, the absorption at 3100–3600 cm^{-1}, which is the absorption due to the vibration of the THX hydroxyl group, remains strong and wide. It can indicate that the interaction between THX and GNP at saturated conditions still exposes the hydroxyl group of THX on the GNP surface (Fig. 6). This is what causes the surface of the GNP to become hydrophilic.

Physical and Chemical Stability Testing

The interaction between G and THX is then tested for physical and chemical stabilities on aqueous media. A physical stability test was investigated by immersing the GNP-THX sample (saturated) in distilled water and then homogenizing it in an ultrasonic bath for 1, 2, 3, and 5 min. Different things are also obtained in this experiment, GNP-THX samples showed good solubility from the sonic time of 1 min and were stable (Fig. 7). It is consistent with the estimated changes in surface morphology of GNP, where the dominant interaction is

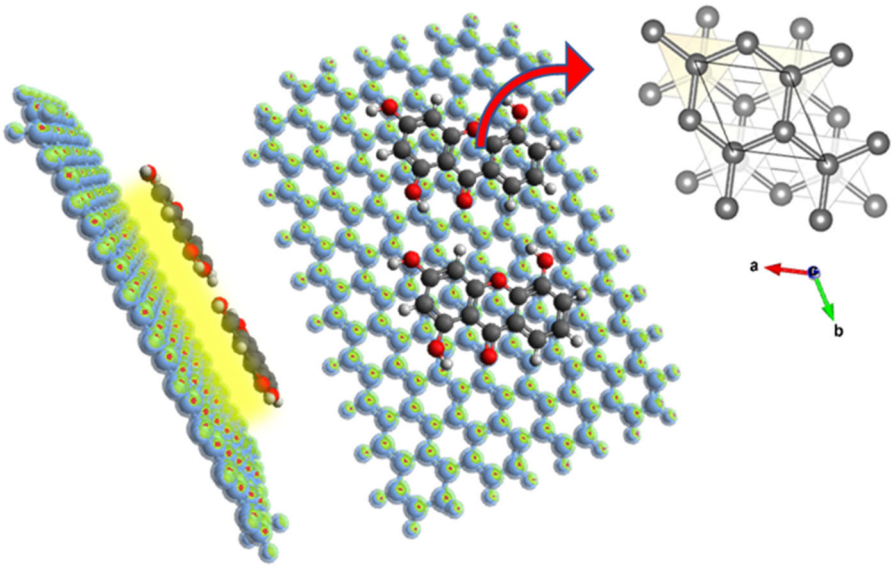

Fig 6. THX interactions on the GNP surface

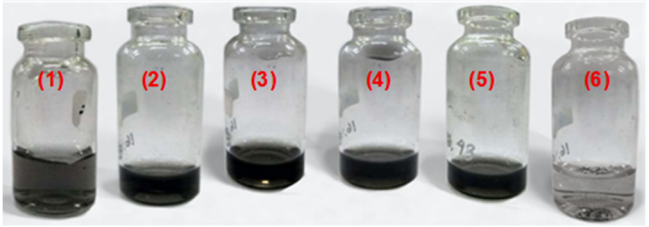

Fig 7. GNP-THX in distilled water that has been given ultrasonic treatment for 1, 2, 3, 4 and 5 min (1, 2, 3, 4 and 5 respectively), GNP (6) (left) and hydrophilicity surface of GNP-THX (right)

by π–π stacking [31] wherein both G and xanthones are in a state of sp^2 hybridization. In contrast, the THX molecule contains hydroxyl, the functional group that is exposed to the G's surface [32]. Therefore, the surface of the G is changed to be more hydrophilic. In addition to using ultrasonic waves, physical stability testing is also carried out by heat triggering using a heating temperature variation of 37–45 °C, based on normal body temperature to above fever related to its purpose as an oral drug. The results that contrast with ultrasonic waves can be seen in the image, where for all heating temperature variations, there is no change in the color of the solution phase as an indication that there is no release of THX molecules, which indicates that GNP-THX is stable to temperature and does not experience denaturation. The van der Waals interactions allow it to be a good energy conductor thanks to the energy transfer from stacking π orbital interactions, which means that GNP-THX becomes a single energy delivery system. The heat energy supplied to the GNP-THX system is continued so that there is no breaking of the interaction between the two molecules [33]. Consequently, unlike previous studies that used ultrasonic waves to release doxorubicin and gold nanoparticles (GNP) in chemotherapy [34], the GNP-THX system will have a more specific mechanism.

In comparison, chemical stability tests were also carried out by placing GNP-THX (saturated) samples at various pH variations, considering the application approach of this material will be used as an oral drug. Hence, it is necessary to consider the pH conditions of the body. The tests showed satisfactory results, where the GNP-THX (saturated) material did not depict signs of denaturation or degradation at acidic to neutral pH. However, GNP-THX material shows denaturation by displaying a color change at alkaline pH or above pH 10 (Fig. 8(a)). The bright yellow color indicates the release of some THX molecules from the GNP surface, and it is due to the presence of strong alkaline media which breaks the π–π stacking interaction between GNP and THX [35], where it is known that the ionic interactions will be more dominant in both GNP and THX in which is indicated by the absence of a precipitate in this condition [36]. This pH stability of GNP-THX (saturated)

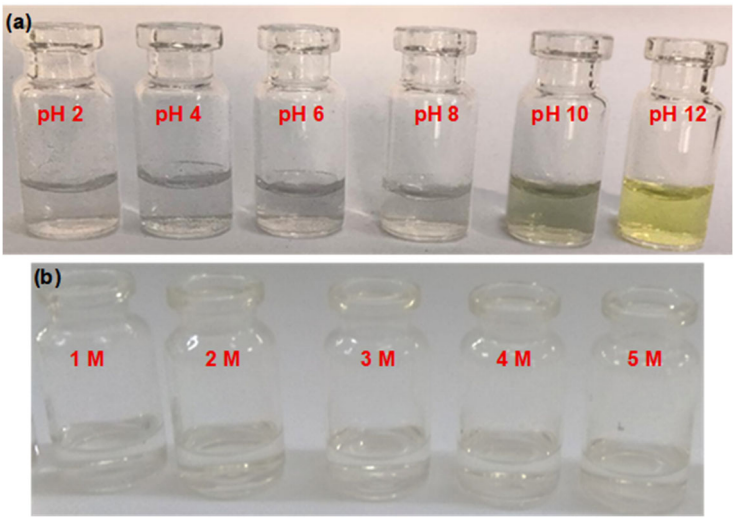

Fig 8. GNP-THX (saturated) in (a) various pH and (b) NaCl concentration

has excellent potential in the development of oral drugs but is targeted for deep parts of the body, such as tumors in specific muscle tissues [37]. This type of drug delivery system is required to remain stable even after passing through the stomach with a very low pH.

Stability to salinity has also been assessed, considering that salinity is an important factor in drug delivery. The results of the stability test on the salt content did not show a qualitative effect (Fig. 8(b)). Consequently, it can be said that the salt content did not affect the release or termination of the THX interaction with G. The cloud of π bonding electrons which can interact with the cation does not affect the release of THX due to the presence of water molecules. Cation-water interactions are preferable to cation-π interactions because of the stronger electrostatic force. The ionic interaction between Na^+ and Cl^- molecules also makes the π-bond cation-bond interaction minimal [38]. Therefore, based on the interaction characteristics, the physical and chemical stability in this study can be used to formulate and control the drug release mechanism.

■ CONCLUSION

To conclude, the overview of the type of interaction between G and drug molecules has an important role, where the interactions formed can change the original characteristics of the material or molecule. XRD data illustrate that GNP saturated by THX molecules can improve its characteristics as G, which is characterized by decreasing the intensity of the (002)-reflection. Moreover, it also explains a decreasing the crystallinity of the G into fewer layers. THX-like molecules can suitably interact with GNP surfaces because of the planar geometry of THX and the π-conjugate system of the three rings. The presence of THX on the GNP surface has changed the GNP characteristics, which are hydrophobic to hydrophilic in the presence of hydroxyl groups on THX. This interaction can be disturbed easily by increasing the pH of the environment. Therefore, the release of THX molecules can be controlled. Therefore, the results of this study show the potential of utilizing G as a drug carrier material for more specific disease targets with a longer drug release time. In addition, further studies need to be conducted to examine the kinetics and dynamics of THX release or similar types of drugs.

■ ACKNOWLEDGMENTS

Financial support for this work comes from the Penelitian Terapan Unggulan Perguruan Tinggi (PTUPT) with contract number 182/SP2H/LT/DRPM/2019 Ministry of Research, Technology, and Higher Education-Indonesia and is gratefully acknowledged.

■ CONFLICT OF INTEREST

The author declares that there is no conflict of interest regarding the publication of this manuscript.

■ AUTHOR CONTRIBUTIONS

Emmy Yuanita was responsible for the original concept and overall study design, and also oversaw the research activities, ensured coordination among team members, and approved the final manuscript for submission. Sirojuttolibin performed the experimental procedures and collected the data. Sudirman carried out the data processing and interpretation. Maulida Septiyana, Ni Komang Tri Dharmayani, and Maria Ulfa assisted in writing the manuscript and provided substantial editorial input. All authors have read and agreed to the published version of the manuscript.

■ REFERENCES

[1] Wang, Y., Wang, H., Liu, F., Wu, X., Xu, J., Cui, H., Wu, Y., Xue, R., Tian, C., Zheng, B., and Yao, W., 2020, Flexible printed circuit board based on graphene/polyimide composites with excellent thermal conductivity and sandwich structure, *Composites, Part A*, 138, 106075.

[2] Gao, F., Liu, K., Cheng, R., and Zhang, Y., 2020, Efficiency enhancement of perovskite solar cells based on graphene-$CuInS_2$ quantum dots composite: The roles for fast electron injection and light harvests, *Appl. Surf. Sci.*, 528, 146560.

[3] Bu, Y., Liang, H., Gao, K., Zhang, B., Zhang, X., Shen, X., Li, H., and Zhang, J., 2020, Wafer-scale fabrication of high-purity reduced graphene oxide films as ultrahigh-frequency capacitors with minimal self-discharge, *Chem. Eng. J.*, 390, 124560.

[4] Wang, D., Zhou, J., Li, J., Jiang, X., Wang, Y., and Gao, F., 2019, Cobalt-boron nanoparticles anchored on graphene as anode of lithium ion batteries, *Chem. Eng. J.*, 360, 271–279.

[5] Lascano, S., Chávez-Vásconez, R., Muñoz-Rojas, D., Aristizabal, J., Arce, B., Parra, C., Acevedo, C., Orellana, N., Reyes-Valenzuela, M., Gotor, F.J., Arévalo, C., and Torres, Y., 2020, Graphene-coated Ti-Nb-Ta-Mn foams: A promising approach towards a suitable biomaterial for bone replacement, *Surf. Coat. Technol.*, 401, 126250.

[6] Shahabi, M., and Raissi, H., 2020, Payload delivery of anticancer drug Tegafur with the assistance of graphene oxide nanosheet during biomembrane penetration: Molecular dynamics simulation survey, *Appl. Surf. Sci.*, 517, 146186.

[7] Song, S., Shen, H., Wang, Y., Chu, X., Xie, J., Zhou, N., and Shen, J., 2020, Biomedical application of graphene: From drug delivery, tumor therapy, to theranostics, *Colloids Surf., B*, 185, 110596.

[8] Jafari, Z., Rad, A.S., Baharfar, R., Asghari, S., and Esfahani, M.R., 2020, Synthesis and application of chitosan/tripolyphosphate/graphene oxide hydrogel as a new drug delivery system for Sumatriptan Succinate, *J. Mol. Liq.*, 315, 113835.

[9] Ruiyi, L., Zaijun, L., Xiulan, S., Jan, J., Lin, L., Zhiguo, G., and Guangli, W., 2020, Graphene quantum dot-rare earth upconversion nanocages with extremely high efficiency of upconversion luminescence, stability and drug loading towards controlled delivery and cancer theranostics, *Chem. Eng. J.*, 382, 122992.

[10] Georgakilas, V., Tiwari, J.N., Kemp, K.C., Perman, J.A., Bourlinos, A.B., Kim, K.S., and Zboril, R., 2016, Noncovalent functionalization of graphene and graphene oxide for energy materials, biosensing, catalytic, and biomedical applications, *Chem. Rev.*, 116 (9), 5464–5519.

[11] Yu, W., Sisi, L., Haiyan, Y., and Jie, L., 2020, Progress in the functional modification of graphene/graphene oxide: A review, *RSC Adv.*, 10 (26), 15328–15345.

[12] Zhang, J., Xu, Y., Cui, L., Fu, A., Yang, W., Barrow, C., and Liu, J., 2015, Mechanical properties of graphene films enhanced by homo-telechelic functionalized polymer fillers via π–π stacking interactions, *Composites, Part A*, 71, 1–8.

[13] Alwarappan, S., Boyapalle, S., Kumar, A., Li, C.Z., and Mohapatra, S., 2012, Comparative study of single-, few-, and multilayered graphene toward enzyme conjugation and electrochemical response, *J. Phys. Chem. C*, 116 (11), 6556–6559.

[14] Haniff Wahid, M., Stroeher, U.H., Eroglu, E., Chen, X., Vimalanathan, K., Raston, C.L., and Boulos, R.A., 2015, Aqueous based synthesis of antimicrobial-decorated graphene, *J. Colloid Interface Sci.*, 443, 88–96.

[15] Chia, J.S.Y., Tan, M.T.T., Khiew, P.S., Chin, J.K., and Siong, C.W., 2015, A bio-electrochemical sensing platform for glucose based on irreversible, non-covalent pi–pi functionalization of graphene produced via a novel, green synthesis method, *Sens. Actuators, B*, 210, 558–565.

[16] Georgakilas, V., Perman, J.A., Tucek, J., and Zboril, R., 2015, Broad family of carbon nanoallotropes: Classification, chemistry, and applications of fullerenes, carbon dots, nanotubes, graphene, nanodiamonds, and combined superstructures, *Chem. Rev.*, 115 (11), 4744–4822.

[17] Yuanita, E., Pranowo, H.D., Siswanta, D., Swasono, R.T., Mustofa, M., Zulkarnain, A.K., Syahri, J., and Jumina, J., 2018, One-pot synthesis, antioxidant activity and toxicity evaluation of some hydroxyxanthones, *Chem. Chem. Technol.*, 12 (3), 290–295.

[18] Zhang, H., Tan, Y., Zhao, L., Wang, L., Fu, N., Zheng, S., and Shen, X., 2020, Anticancer activity of dietary xanthone α-mangostin against hepatocellular carcinoma by inhibition of STAT3 signaling via stabilization of SHP1, *Cell Death Dis.*, 11 (1), 63.

[19] Yuanita, E., Sudarma, I.M., Sudewiningsih, N.M., Syahri, J., Dharmayani, N.K.T., Sudirman, S., Ulfa, M., and Sumarlan, I., 2020, Antibacterial activity and molecular docking studies of series hydroxyxanthone, *AIP Conf. Proc.*, 2243 (1), 020032

[20] Syahri, J., Yuanita, E., Nurohmah, B.A., Wathon, M.H., Syafri, R., Armunanto, R., and Purwono, B., 2017, Xanthone as antimalarial: QSAR analysis, synthesis, molecular docking and in-vitro antimalarial evaluation, *Orient. J. Chem.*, 33 (1), 29–40.

[21] Vrbanac, J., and Slauter, R., 2017, "Chapter 3 - ADME in Drug Discovery" in *A Comprehensive Guide to Toxicology in Nonclinical Drug Development (Second Edition)*, Eds. Faqi, A.S., Academic Press, Boston, US, 39–67.

[22] Kim, J., Han, J.W., and Yamada, Y., 2021, Heptagons in the basal plane of graphene nanoflakes analyzed by simulated X-ray photoelectron spectroscopy, *ACS Omega*, 6 (3), 2389–2395.

[23] Zhang, X.F., Liu, S.P., and Shao, X.N., 2013, Noncovalent binding of xanthene and phthalocyanine dyes with graphene sheets: The effect of the molecular structure revealed by a photophysical study, *Spectrochim. Acta, Part A*, 113, 92–99.

[24] Evans, I.R., Howard, J.A.K., Šavikin-Fodulović, K., and Menković, N., 2004, Isogentisin (1,3-dihydroxy-7-methoxyxanthone), *Acta Crystallogr., Sect. E:Crystallogr. Commun.*, 60 (9), 1557-1559.

[25] Yu, S., Wang, X., Ai, Y., Tan, X., Hayat, T., Hu, W., and Wang, X., 2016, Experimental and theoretical studies on competitive adsorption of aromatic compounds on reduced graphene oxides, *J. Mater. Chem. A*, 4 (15), 5654–5662.

[26] Shiva, K., Ramakrishna Matte, H.S.S., Rajendra, H.B., Bhattacharyya, A.J., and Rao, C.N.R., 2013, Employing synergistic interactions between few-layer WS_2 and reduced graphene oxide to improve lithium storage, cyclability and rate capability of Li-ion batteries, *Nano Energy*, 2 (5), 787–793.

[27] Huber, R.G., Margreiter, M.A., Fuchs, J.E., von Grafenstein, S., Tautermann, C.S., Liedl, K.R., and Fox, T., 2014, Heteroaromatic π-stacking energy landscapes, *J. Chem. Inf. Model.*, 54 (5), 1371–1379.

[28] Johra, F.T., Lee, J.W., and Jung, W.G., 2014, Facile and safe graphene preparation on solution based platform, *J. Ind. Eng. Chem.*, 20 (5), 2883–2887.

[29] Janiak, C., 2000, A critical account on π–π stacking in metal complexes with aromatic nitrogen-containing ligands, *J. Chem. Soc., Dalton Trans.*, (21), 3885–3896.

[30] Patel, C.R.P., Tripathi, P., Vishwakarma, A.K., Talat, M., Soni, P.K., Yadav, T.P., and Srivastava, O.N., 2018, Enhanced hydrogen generation by water electrolysis employing carbon nano-structure composites, *Int. J. Hydrogen Energy*, 43 (6), 3180–3189.

[31] Han, X., Kong, H., Chen, T., Gao, J., Zhao, Y., Sang, Y., and Hu, G., 2021, Effect of π–π stacking interfacial interaction on the properties of graphene/poly(Styrene-b-isoprene-b-styrene) composites, *Nanomaterials*, 11 (9), 2158.

[32] Zainal-Abidin, M.H., Hayyan, M., Ngoh, G.C., and

Wong, W.F., 2020, Doxorubicin loading on functional graphene as a promising nanocarrier using ternary deep eutectic solvent systems, *ACS Omega*, 5 (3), 1656–1668.

[33] Guo, Y., Luo, X.P., Zhang, Z., Merabia, S., Nomura, M., and Volz, S., 2023, Basal-plane heat transport in graphite thin films, *Phys. Rev. B*, 107 (19), 195430.

[34] Hornsby, T.K., Kashkooli, F.M., Jakhmola, A., Kolios, M.C., and Tavakkoli, J., 2023, Kinetic modelling of ultrasound-triggered chemotherapeutic drug release from the surface of gold nanoparticles, *Sci. Rep.*, 13 (1), 21301.

[35] Zhan, J., Lei, Z., and Zhang, Y., 2022, Non-covalent interactions of graphene surface: Mechanisms and applications, *Chem*, 8 (4), 947–979.

[36] Zhan, C., Cerón, M.R., Hawks, S.A., Otani, M., Wood, B.C., Pham, T.A., Stadermann, M., and Campbell, P.G., 2019, Specific ion effects at graphitic interfaces, *Nat. Commun.*, 10 (1), 4858.

[37] Zelepukin, I.V., Griaznova, O.Y., Shevchenko, K.G., Ivanov, A.V., Baidyuk, E.V., Serejnikova, N.B., Volovetskiy, A.B., Deyev, S.M., and Zvyagin, A.V., 2022, Flash drug release from nanoparticles accumulated in the targeted blood vessels facilitates the tumour treatment, *Nat. Commun.*, 13 (1), 6910.

[38] Fernández, A.C.R., and Castellani, N.J., 2020, Dipole moment effects in dopamine/N-doped-graphene systems, *Surf. Sci.*, 693, 121546.